

Methods of determining the contact between a probe and a surface under scanning electron microscopy

C.-H. Nien, C. H. Tsai, K. Y. Shin, and W. B. Jian

Citation: [Review of Scientific Instruments](#) **77**, 103709 (2006); doi: 10.1063/1.2360883

View online: <http://dx.doi.org/10.1063/1.2360883>

View Table of Contents: <http://scitation.aip.org/content/aip/journal/rsi/77/10?ver=pdfcov>

Published by the [AIP Publishing](#)

Articles you may be interested in

[Silicon photodiodes for low-voltage electron detection in scanning electron microscopy and electron beam lithography](#)

J. Vac. Sci. Technol. B **24**, 2951 (2006); 10.1116/1.2363405

[Shape dependent thermal effects in apertured fiber probes for scanning near-field optical microscopy](#)

J. Appl. Phys. **99**, 084303 (2006); 10.1063/1.2188250

[High-speed and high-precision deflectors applied in electron beam lithography system based on scanning electron microscopy](#)


J. Vac. Sci. Technol. B **22**, 3557 (2004); 10.1116/1.1813454

[Scanning tunneling microscopy studies of the Fe₃O₄ \(001\) surface using antiferromagnetic probes](#)


J. Appl. Phys. **93**, 7142 (2003); 10.1063/1.1556199

[Observation of selective thermal desorption of electron stimulated SiO₂ with a combined scanning reflection electron microscope/scanning tunneling microscope](#)

J. Appl. Phys. **82**, 639 (1997); 10.1063/1.365592



**Does your research require low temperatures? Contact Janis today.
Our engineers will assist you in choosing the best system for your application.**



10 mK to 800 K **LHe/LN₂ Cryostats**
Cryocoolers **Magnet Systems**
Dilution Refrigerator Systems
Micro-manipulated Probe Stations

sales@janis.com **www.janis.com**
Click to view our product web page.

Methods of determining the contact between a probe and a surface under scanning electron microscopy

C.-H. Nien^{a)}

Department of Physics, National Central University, Zhongli, Touyuan 320, Taiwan

C. H. Tsai and K. Y. Shin

Department of Engineering and System Science, National Tsing Hua University, Hsinchu 300, Taiwan

W. B. Jian

Department of Electrophysics, National Chiao Tung University, Hsinchu 300, Taiwan

(Received 28 June 2006; accepted 10 September 2006; published online 24 October 2006)

Based on the charging effect common to various kinds of electron microscopy, we have developed novel methods of determining “when” and “where” a probe starts to contact an electrically isolated surface. The touchdown of an electrically grounded probe leads to an acute change in the imaging contrast of the contacted surface, which also causes a rapid jump (ranging from a few to tens of picoamperes) of the grounding current. Thus, the detection of contact can be carried out in both qualitative and quantitative manners, providing a basis for establishing relevant standard procedures. In addition, we have achieved the spatial mapping of the contact point(s) using a specially designed lithographical pattern with two mutually vertical sets of parallel conductive lines. The precision of this mapping technique is simply determined by the pitch of parallel lines, which can be as small as the capability achievable in e-beam lithography. A possible “one-probe” version of the electrical characterization is also discussed with the same underlying principle, which may turn out to be indispensable for various studies and applications of nanostructures. Further development along this track is promising to realize an instrumentally simple version of “scanning electron spectroscopy” with various modes. © 2006 American Institute of Physics.

[DOI: [10.1063/1.2360883](https://doi.org/10.1063/1.2360883)]

I. INTRODUCTION

The evolution of scanning electron microscopy (SEM) has gone through a long way to bring us a versatile tool for microscopic investigation. In addition to the basic function of imaging microscopic structures down to nanometer scale, SEM has been further developed by many efforts to possess various optional modes of microanalysis, most of which demand some sophisticated devices.¹ In contrast, it was not until a few years ago when multiprobe systems operated inside SEM started to gain an increasing attention from the community of both nanoscience and nanotechnology.² On the one hand, SEM-based multiprobe systems are probably the most literal tools of nanomanipulation for scientists. The relative ease of sample preparation and the manipulation with a real-time watching also contribute major advantages of this development over other competitive approaches based on the transmission electron microscope³ (TEM) and the atomic force microscope (AFM),⁴ respectively. Among the reported scientific achievements based on the SEM-based multiprobe systems are the attempts to manufacture nanoscale structures [e.g., the attachment of carbon nanotubes (CNTs) onto a tip for scanning probe microscopes⁵ (SPMs) or field-emission properties]⁶ and the efforts to study the mechanical or electrical properties of nanostructures (e.g., the

conductivity of nanowires by the standard four-probe measurement).⁷ On the other hand, more and more routine tasks (e.g., the quality control of products) for engineers in the semiconductor industry have also become dependent upon the SEM-based multiprobe systems to serve as the electrical probing tool for their submicron electronics.⁸

At this stage, however, some basic techniques relevant to the performance of this advanced instrument are still far from maturity. For instance, the establishment of contact between the probes and the target features on the substrate surface, a vital step when this instrument acts as an electrical probing system, still relies greatly on a primitive trial and error. To the best of our knowledge, the current way of running a SEM-based multiprobe system is to keep a sharp tip of the probe in some tilted orientation all the time, so that one can track the very end of the probe (which is presumed to be the contact point) by watching the real-time SEM image.⁶ As for the moment of contact, it may not be sensed until some visible lateral slips or damages occur.

In this article, we present some simple but effective solutions to these problems for a multiprobe system operated inside SEM. Based on the charging effect common to various kinds of electron microscopy,¹ we demonstrate our methods of determining “when” and “where” a probe starts to contact an electrically isolated surface. A possible “one-probe” ver-

^{a)} Author to whom correspondence should be addressed; electronic mail: chnien@phy.ncu.edu.tw

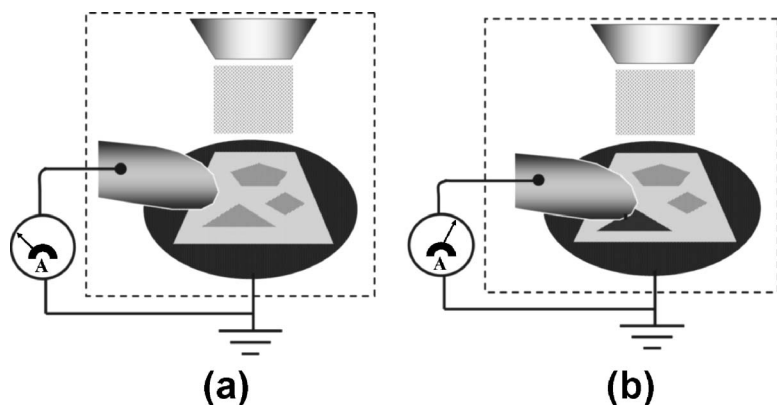


FIG. 1. The basic configuration and the working principle of our methods. Three conductive samples are electrically isolated from the ground, and the conductive probe is connected to the ground through an ammeter. (a) The “charging effect” of all samples (due to their electrical isolation from the ground) upon imaging by the scanned electron beam. It causes a poor imaging contrast of all samples. (b) A sensible change in the imaging contrast of the contacted sample surface and the corresponding change of the “grounding current” upon touchdown of the probe.

sion of the electrical characterization with the same underlying principle is also explored for its potential applications to the studies of nanostructures.

II. PRINCIPLE OF OPERATION

Instead of trying to avoid the “charging effect” at the first place by getting the samples grounded in one way or another, we first keep the samples electrically isolated from the ground (i.e., electrically disconnected from the sample holder) while the probe is connected to the ground through an ammeter, as depicted in Fig. 1. Upon imaging by the scanned electron beam, the samples will suffer the expected charging effect due to their electrical isolation from the ground, resulting in a poor contrast of the samples in the image, as depicted in Fig. 1(a). This situation will change as soon as the electrically grounded probe is brought to touch a sample, leading to the effective depletion of previously accumulated charges. Depending on the electrical property of this sample (among other factors), the event of contact will then cause a corresponding change of contrast to various extents, as depicted in Fig. 1(b). Furthermore, we also expect a corresponding change (upon contact) for the “grounding current,” which is the flow of electrons between the sample surface and the ground as a result of the continuous impingement of the electron beam. Note that the grounding current bypasses the conventional way (via the sample holder) and goes through an ammeter in the configuration of our methods, which turns out to share the same underlying concept with a long recognized mode (usually termed the “specimen current” or “adsorbed current”) available for SEM-based microanalysis.¹ Nevertheless, the temporary connection of the sample to the ground through a maneuverable probe, a technical feature unique to our approach, is likely to provide greater opportunities of various novel techniques for nanoscale applications.

In addition to determining when a probe starts to contact an electrically isolated surface, we have also developed a method to answer the question about where the contact site(s) is (are) located. Unlike the relative mapping (to the imaged field itself only) as provided by a scanning probe microscope (SPM), our method allows the absolute location(s) of the contact point(s) to be mapped with respect to either the sample surface or the probe itself. Again, our method of mapping the contact point(s) takes advantage of the charging effect with a specially designed lithographical

pattern (to serve as the tool of calibration). Ideally, the most straightforward structure for this pattern to function is probably as complex as the conceptual design depicted in Fig. 2(a), where two sets of parallel conductive lines are lithographically fabricated (on top of the same surface of interest or a surface with the same orientation) so that the lines belonging to one set cross on top of those belonging to the other. Moreover, these conductive lines are electrically isolated from the ground as well as from each other (say, by sufficiently thick layers of insulating oxide). In the case of a single contact site, the touchdown of the probe onto this pattern will change the imaging contrast of two crossed lines, indicating the location of the contact point [as illustrated in Fig. 2(b)]. Note that the identified contact point with respect to the probe itself will remain the same as long as the probe keeps its orientation while exploring a sufficiently flat area having a common surface normal with the calibrating pattern. In principle, we can therefore achieve a precise contact with the spatial uncertainty determined solely by the pitch of this calibrating pattern (regardless of how blunt the probe might be). As a result, the requirement of a sharp tip can now be eliminated for whatever applications involving contact of the probe with a sufficiently flat surface.

Having considered the relatively high demand of labor and technical skill for fabricating the conceptual version of our calibrating pattern, we are further committed to propose a more practical version with a much simpler structure, resulting in a lower failure rate of fabrication and a better durability. The pattern of this alternative version is also composed of two sets of parallel conductive lines, the common direction of which in one set is vertical to that in the other. However, these two sets of lines are now patterned side by side [as depicted in Fig. 2(c)] instead of crossing each other with an insulating layer in between. Consequently, the mapping procedure will now involve the touchdown of the probe onto one set of parallel lines to determine the first coordinate of the contact point (s), followed by the touchdown onto the other set of parallel lines to determine the second coordinate. This two-step procedure (instead of only one step for the conceptual version) of mapping can be regarded as a little price to pay in operation for saving a lot of efforts in fabricating the corresponding pattern.

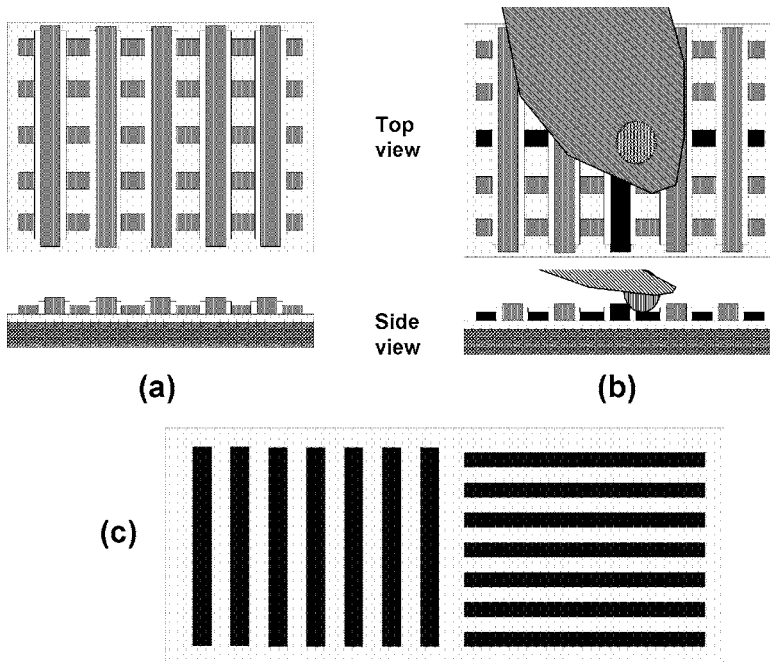


FIG. 2. The method of mapping the contact point(s) with lithographically fabricated patterns. (a) The conceptual version of our calibrating patterns comprises two sets of parallel conductive lines. The lines belonging to one set cross on top of those belonging to the other. Moreover, these conductive lines are electrically isolated from the ground as well as from each other (say, by sufficiently thick layers of insulating oxide). (b) The function of the conceptual calibrating pattern is illustrated. In the case of a single contact site, the touchdown of the probe onto this pattern will change the imaging contrast of two crossed lines, implying the location of the contact point (as indicated by the dashed circle). (c) The practical version of our calibrating pattern comprises two sets of parallel conductive lines side by side. The common direction of the lines in one set is vertical to that in the other.

III. EXPERIMENTAL RESULTS

The SEM-based multiprobe nanoelectronics measurement system in this work is composed of JOEL-7000 field-emission SEM equipped with a four-nanoprobe system (manufactured by Kammrath & Weiss, Germany). The measurement of the grounding current is done by a Keithley 4200-SCS to serve as the ammeter with a resolution better than 0.1 pA.

We have followed the standard procedure of e-beam lithography to fabricate a calibrating pattern with our practical version. In this testing pattern, the conductive lines with a pitch of 500 nm were made of gold strips of 100 nm thick and 200 nm wide deposited onto an insulating oxide layer (of 1000 nm thick) on top of silicon wafer. A square pattern (with a size of $400 \times 400 \mu\text{m}^2$) of gold film was also fabricated in the same way to test our methods of detecting the events of contact.

An example of determining the contact of probes with our method is illustrated in Fig. 3, where the surface feature is a square pattern of gold film (of 100 nm thick, with a size of $400 \times 400 \mu\text{m}^2$) deposited onto an insulating oxide layer (of 1000 nm thick) on top of a silicon wafer. As clearly shown in Figs. 3(a) and 3(b) by SEM images, the touchdown of an electrically grounded probe leads to an acute change in the imaging contrast of the contacted surface (i.e., the conductive gold square). We have also confirmed the existence of the corresponding change (approximately a few picoamperes) in the grounding current, as illustrated in Fig. 3(c) for two times of touchdown. In this way, the same event of contact that induces a sudden change of the imaging contrast in Fig. 3(b) is also found to cause a rapid jump (approximately a few picoamperes) of the grounding current in Fig. 3(c). Thus, the detection of contact can now be carried out in both qualitative and quantitative manners. It was also noticed that the mechanism of moving the probe in commercially available multiprobe systems may require some improvement to

meet the need of nanoscale manipulation. This is vividly shown by the overshooting spikes in Fig. 3(c), which are attributed to a rough touchdown of the probe.

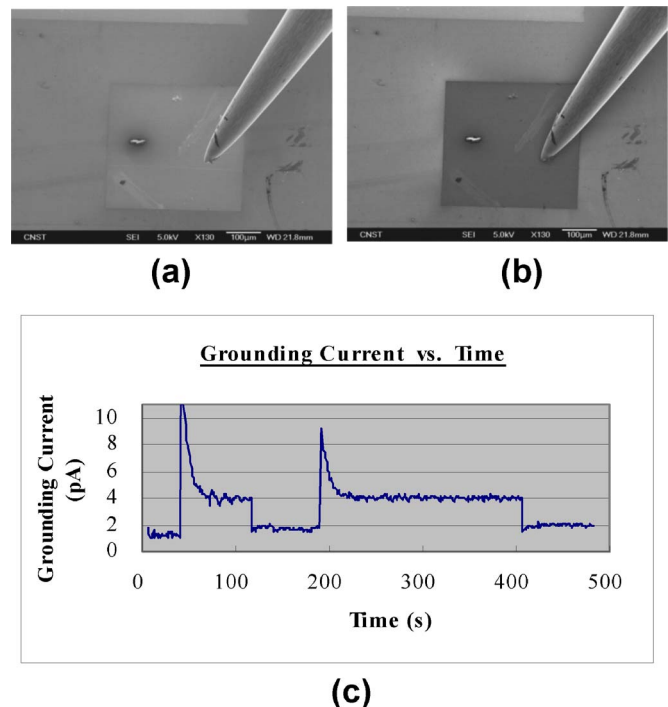


FIG. 3. (Color online) A test of our method to determine the contact of the probe with a square pattern of gold film (of 100 nm thick, with a size of $400 \times 400 \mu\text{m}^2$). The film was deposited onto an insulating oxide layer (of 1000 nm thick) on top of a silicon wafer. SEM images (a) before and (b) after the touchdown of the probe show an acute change in the imaging contrast of the contacted surface. (c) The measured “grounding current” as a function of time, showing a corresponding change (approximately a few picoamperes) upon contact for two times of touchdown. The two plateaus (~ 4 pA) correspond to two times of stationary contact. Notice that the overshooting spikes resulted from a rough touchdown of the probe due to the unsatisfactory mechanisms of moving the probe.

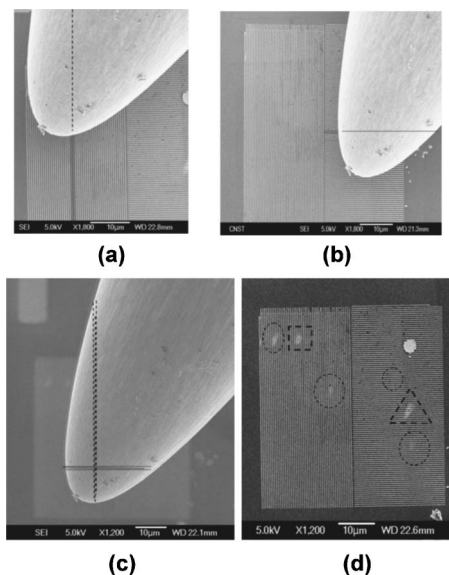


FIG. 4. A test for our method of mapping the contact point(s) with a practical version of the calibrating pattern. SEM images (a) and (b) show the sequential touchdown of the probe onto each set of the lines (by moving around both the probe and the calibrating pattern), causing a drastic change of the imaging contrast for some line(s) to determine the corresponding coordinate of the contact point(s). Extrapolated from these “lighted lines” on the calibrating pattern, the corresponding dashed strips indicate the final identification of the possible contacted regions on the probe. (c) A summary of the experimental data from six different runs of touchdown in a statistical fashion. Six dashed strips extrapolated from the lighted lines in all events of touchdown are plotted together on the probe. Essentially, three lines of each set coincide with one another very well. The detached calibrating pattern serves as irrelevant background in this image. (d) An overview of the calibrating pattern after six runs of touchdown. Note that the six damaged sites due to the unsatisfactorily rough touchdown of various extents are enclosed by six dashed boxes of various shapes. In particular, the thick dashed square and triangle enclose the contact sites corresponding to the events of (a) and (b), respectively.

As for our method of mapping the contact point(s) with a practical version of the calibrating pattern, a typical example is demonstrated in Figs. 4(a) and 4(b), where the parallel conductive lines (with a pitch of 500 nm) in our calibrating pattern were composed of gold strips (of 100 nm thick and 200 nm wide) deposited onto an insulating oxide layer (of 1000 nm thick) on top of a silicon wafer. In this two-step procedure, the touchdown of the probe onto each set of lines causes a drastic change of the imaging contrast for some line(s) to determine the corresponding coordinate of the contact point(s) with respect to the probe itself. For example, Figs. 4(a) and 4(b) illustrate two consecutive runs of touchdown (by moving around both the probe and the surface) onto the two complementary portions of the calibrating pattern, determining the X coordinate and Y coordinate of the same contact point on the probe, respectively. With the detached calibrating pattern as irrelevant background, Fig. 4(c) summarizes the experimental data from six different runs of touchdown in a statistical fashion, where the locations of “lighted lines” (i.e., lines with visible change in their imaging contrast) are extrapolated and mapped together by dashed strips onto the probe. Since the probe has always been kept in the same orientation relative to all surfaces of interest, the remarkable coincidence of the contact points [i.e., the crossing points of these dashed strips in Fig. 4(c)]

demonstrates the reliability of this mapping technique. An overview of the calibrating pattern after six runs of touchdown is also shown in Fig. 4(d), where the damaged sites (as enclosed by dashed boxes of various shapes) can be used to identify the exact location (with respect to the surface) of each touchdown. For example, the thick dashed square and triangle enclose the contact sites corresponding to Figs. 4(a) and 4(b), respectively. Again, the variation of the resultant damages on the pattern is likely to come from unsatisfactory mechanisms of moving the probe, causing a rough touchdown to various extents. On the other hand, the damaged pattern indeed provides a convincing evidence of how our methods work.

In conjunction with a sensible change of the imaging contrast, a measurable change (approximately a few tens of picoamperes) of the grounding current was also detected upon the touchdown of the probe onto the calibrating pattern, as illustrated in Fig. 5(a). In contrast to the overshooting spike upon the first touchdown, the second one depicts a much smoother rising of the grounding current. What made the difference is just a little practice of moving the probe while the grounding current is being monitored. This demonstrates the need for a quantitative way of determining the contact in a real-time fashion. As for the measured results, we noticed [by comparing Figs. 3(c) and 5(b)] that the change of the steady-state grounding current seems to increase upon the reduction of the imaged area, which may not be comprehensible at a glance. This observation addresses the issue of what factors determine the magnitude of the change in the steady-state grounding current upon the event of touchdown. Among the significant factors we have verified experimentally are the energy and the flux of the electron beam. As shown in Figs. 5(b) and 5(c), we have observed a monotonically linear behavior for the overall relation between the steady-state grounding current and either factor. It remains to be a subject of further study about how exactly these characteristics are related to the underlying causes such as the surface properties.

IV. DISCUSSION

As demonstrated in the previous section, our methods to detect the contact of probes can be carried out in both qualitative and quantitative fashions. Being aware of the rapidly growing community associated with SEM-based multiprobe systems, we are convinced that the quantitative method to determine the contact (in terms of the grounding current) may help some standard procedures to be established. As a result, different measurements with SEM-based multiprobe systems can be more reliable for comparison.

On the other hand, our method of mapping the contact sites can be interpreted as the tracking of the invisible contact spots by the extension of the imaging contrast along conductive lines. Remarkably, we can also apply the same underlying principle in a reversed fashion. If a contact has been established between the grounded probe and a designated conductive line, the visible discontinuity of the imaging contrast along this line will then reveal the failure sites of electrical continuity. This failure mapping technique allows

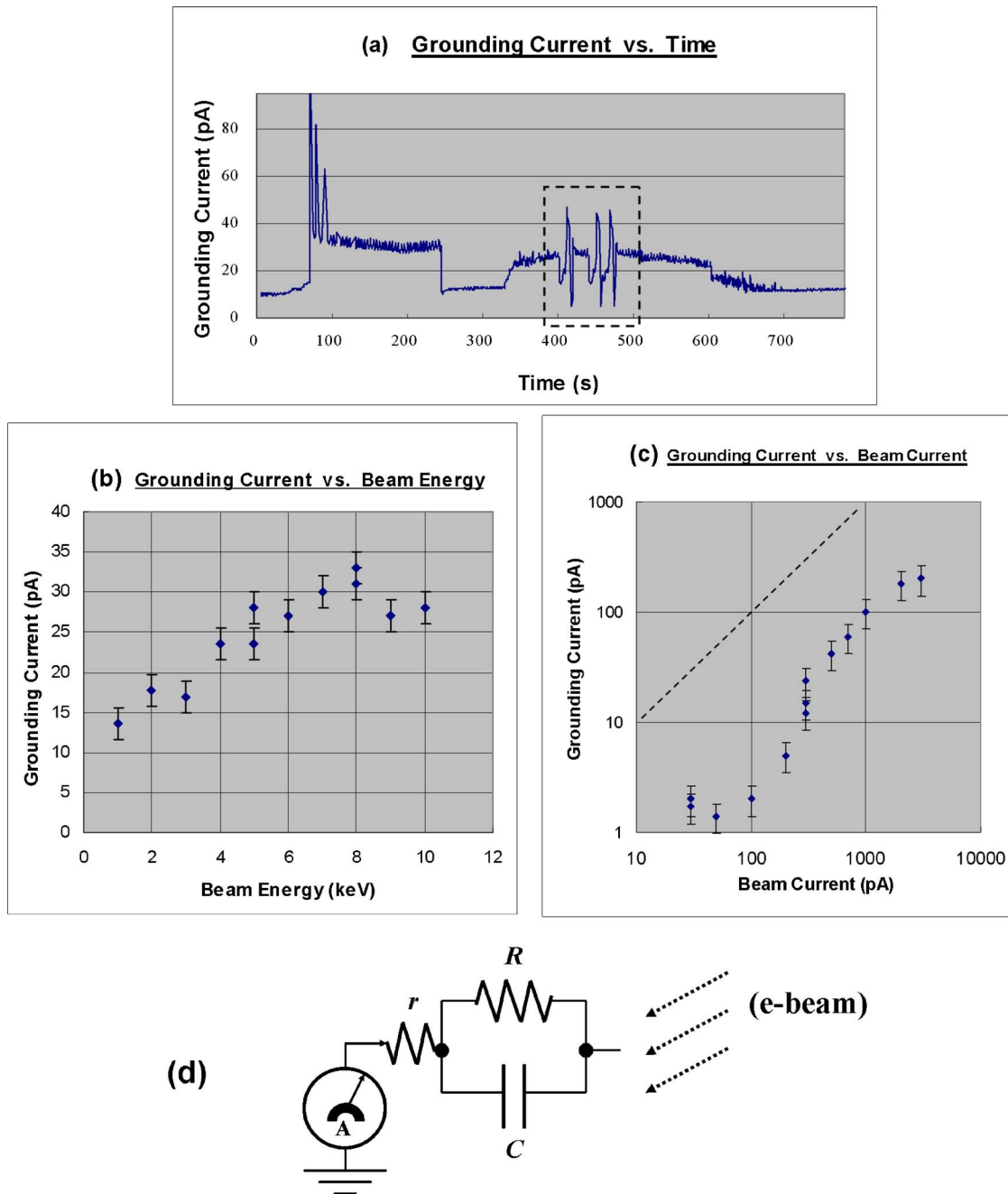


FIG. 5. (Color online) Quantitative analysis of the measured grounding current. (a) The grounding current is plotted as a function of time for the touchdown of the probe onto the calibrating pattern twice. Note that a wild fluctuation in the grounding current occurs whenever a SEM image is being recorded by a slow scan, as highlighted by a dashed box. (b) The steady-state grounding current upon contact is recorded as a function of the beam energy in a linear plot. The beam current was set to 300 pA. (c) The steady-state grounding current upon contact is recorded as a function of the beam current in a log-log plot. The dashed line corresponds to $I(\text{ground})=I(\text{beam})$. The beam energy was set to 5 keV. In all experiments in (b) and (c), the emission current of the electron source was set to 39 μA , and the magnification was 1300. (d) A proposed model for the imaged sample is composed of an equivalent R - C parallel circuit. A possible contact resistance r between the probe and the surface is also taken into account.

spatial designation of the desired target to examine, which may provide a timely solution to the ever increasing challenge of failure analysis in the semiconductor industry dealing with more and more compact nanoelectronics.⁹

In our attempt to understand the experimental results in a quantitative manner, we have modeled the imaged sample by assuming an equivalent R - C parallel circuit (i.e., a resistor of resistance R and a capacitor of capacitance C in parallel), as depicted in Fig. 5(d). A contact resistance r between the probe and the surface is also taken into account. As an ex-

ample of how this model advances our analysis, let us examine the measurement of the steady-state grounding current versus the flux of the electron beam. We assume that the continuous impingement of the electron beam can be regarded as the driving force (by establishing a nonuniform spatial distribution of charge across the sample) to build up a steady-state bias voltage across the resistor R as well as the capacitor C . In spite of the seemingly complicated mechanisms involved in the SEM imaging process, the built steady-state bias voltage is probably related to the flux of the

electron beam in a monotonic fashion. If we further assume an ideal case where this monotonic relation can be approximated by a constant proportionality (i.e., $V/I(\text{beam}) \equiv k = \text{const}$) within a range of the impinged electron flux, the measurement of the characteristic I - V curve in this range is then equivalent to the measurement of the steady-state grounding current versus the impinged electron flux up to a proportional constant [i.e., $R = V/I(\text{ground}) = k \times I(\text{beam})/I(\text{ground})$ with a constant k for this ideal case]. Since there can be a background value of the grounding current that has nothing to do with the contact of the probe with the sample, $I(\text{ground})$ in the above formula actually corresponds to the “change” in the steady-state grounding current upon the event of touchdown. This background value may be reduced by adjusting the impinged region of the electron beam.

Alternatively speaking, having the continuous impingement of the electron beam to serve as the driving force (in place of an externally applied bias voltage), one may be able to characterize the electrical properties of an electrically isolated object through the proper contact with a grounded probe, followed by the measurement of the grounding current as a function of the beam energy and/or flux. Notice that this one-probe approach may become indispensable for nanostructures, as the conventional four-probe electrical measurement is unlikely to be applicable in these cases. On the one hand, there is often limited space on a nanostructure to establish four separate contacts for the conventional version of the electrical measurement. On the other hand, the surface properties are likely to play a dominant role in the case of a nanostructure, suggesting a possibility to define alternative ways of measuring the electrical properties.

In the one-probe electrical characterization based on our methods, the grounded probe can be viewed to play the role of designating an individual object (among other electrically isolated ones) by a local contact for the charging effect to be “turned off.” This is followed by the measurement of the grounding current (through the probe) as a function of a parameter of interest to run the electrical characterization (in an unconventional fashion) for this designated nanostructure. Therefore, the basic configuration (as depicted in Fig. 1) we adopted to determine the contact of probes may also allow us to study the electrical properties of individual nanostructures one at a time. Note that the great opportunity of “individual study” is not possible if the grounding current is collected through the sample holder instead,¹⁰ as we cannot selectively measure the contribution of a specified feature to the grounding current in that case. As for the required electrical isolation of the surface features from the ground, one may be able to achieve “tenability” by some lithographical designs along with the so-called field effect (say, by applying a proper “gate voltage”).

In comparing the relation between the scanning tunneling microscopy (STM) and the scanning tunneling spectroscopy (STS),¹¹ our one-probe approach to the electrical characterization seems more promising for the corresponding technique called “scanning electron spectroscopy (SES)” to be established in an instrumentally simple fashion. The basic features of SES to be expected include at least one mode of

spectroscopic measurement (e.g., I - V characteristic) with a spatial resolution close to that of SEM. In addition to the energy and the flux of the electron beam as promising independent variables for this technique, further studies may also find ways for other parameters (e.g., the operated magnification) to join the available SES modes for nanoscale research.

V. SUMMARY

In summary, we have developed simple but effective methods of determining when and where a probe starts to contact an electrically isolated surface. Based on the charging effect common to various kinds of electron microscopy, these techniques are designed for a multiprobe system operated inside a scanning electron microscope (SEM). As conceptually predicted and experimentally confirmed, a touchdown of an electrically grounded probe leads to an acute change in the imaging contrast of the contacted surface, which also causes a rapid jump of the grounding current (ranging from a few to tens of picoamperes). Thus, the detection of contact can be carried out in both qualitative and quantitative manners, providing a basis for establishing relevant standard procedures.

In addition, we have achieved the spatial mapping of the contact point(s) with respect to the probe itself (unlike what SPM is restricted). This involves a specially designed lithographical pattern with two mutually vertical sets of parallel conductive lines. The precision of this mapping technique is simply determined by the pitch of these parallel lines, which can be as small as the capability achievable in e-beam lithography. Remarkably, one can also apply the reversed working principle to reveal the failure sites of electrical continuity in a complicated circuit. This mapping technique may therefore provide an effective solution to the upcoming challenge of failure analysis for nanoelectronics in the semiconductor industry.

An equivalent R - C parallel circuit was examined to model the imaged sample in our attempt at a quantitative analysis of the experimental results. We have also discussed a possible one-probe version of the electrical characterization based on the same underlying principle, which may turn out to be indispensable for various studies and applications of nanostructures. Further development along this track is promising to realize an instrumentally simple version of scanning electron spectroscopy (SES) with various modes.

ACKNOWLEDGMENT

This work was supported by the Center of Nano-Science and Technology (CNST) of the University System of Taiwan (UST).

¹ Among comprehensive books to provide an overview is L. Reimer, *Scanning Electron Microscopy*, Springer Series in Optical Sciences Vol. 45 (Springer, Berlin, 1985).

² M.-F. Yu, O. Lourie, M. J. Dyer, K. Moloni, T. F. Kelly, and R. S. Ruoff, *Science* **287**, 637 (2000).

³ T. Kuzumaki, H. Sawada, H. Ichinose, Y. Horiike, and T. Kizuka, *Appl. Phys. Lett.* **79**, 4580 (2003).

⁴ H. W. C. Postma, A. Sellmeijer, and C. Dekker, *Adv. Mater. (Weinheim, Ger.)* **12**, 1299 (2000).

- ⁵S.-D. Tzeng, C.-L. Wu, Y.-C. You, T. T. Chen, and S. Gwo, *Appl. Phys. Lett.* **81**, 5042 (2002).
- ⁶K. S. Kim, S. C. Lim, I. B. Lee, K. H. An, D. J. Bae, S. Choi, J.-E. Yoo, and Y. H. Lee, *Rev. Sci. Instrum.* **74**, 4021 (2003).
- ⁷R. Gupta, R. E. Stallcup II, and M. in het Panhuis, *Nanotechnology* **16**, 1707 (2005).
- ⁸S. Tiwari and H. Tokumoto, *Report on Japan-US Symposium on Tools and Metrology for NanoTechnology* (Cornell University, Ithaca, 2003).
- ⁹J. Ouellette, *Ind. Phys.* **4**, 11 (1998).
- ¹⁰J. Liebault, K. Zarbout, D. Moya-Siesse, J. Bernardini, and G. Moya, *Appl. Surf. Sci.* **212–213**, 809 (2003).
- ¹¹Among comprehensive books to provide an overview is: C. J. Chen, *Introduction to Scanning Tunneling Microscopy*, Oxford Series in Optical and Imaging Sciences Vol. 4 (Oxford University Press, New York, 1993).